Arch. Metall. Mater. **63** (2018), 1, 247-256

DOI: 10.24425/118935

M. MERZOUG*#, A. BOULENOUAR*, B. BOUCHOUICHA*, M. SERRIER**, M. MAZARI*

EFFECTS OF WELDING PARAMETERS ON FSSW: EXPERIMENTAL AND NUMERICAL STUDY

In this paper, the Aluminum A6060-T5 plates of thickness 2 mm was friction stir spot welded (FSSW), and the effects of welding parameters (rotation speed, plunge speed and distance from the center of pin) on the temperature variation of the joints were investigated. The experimental design method is used to investigate the effects of welding parameters in order to achieve an optimization of the FSSW process. This optimization allows the development of experimental results and may help to better understand the complexity of the phenomena resulting from contact parts/tool during the stirring process.

Keywords: FSSW, penetration, rotation of the tool, temperature, design of experiments

1. Introduction

As a relatively new manufacturing process, there is limited published research work on FSSW process as compared to friction stir welding (FSW). Several works, however, have been discussed in symposia and conferences. Lin and al. [1] investigated microstructures and failure mechanisms of FSSW in aluminum 6111-T4 based on experimental observations. Feng and al. [2] reported about their feasibility study of FSSW in advanced high-strength steels such as AHSS. Mitlin and al. [3] conducted experiments to investigate structure-properties relations in spot friction welded 6111 T4 Aluminum. More recent works on FSSW include. Pan and al. [4] on sheet aluminum joining and Sakano and al. [5] on development of FSSW robot system for automobile industry. Mechanical properties are critical for an FSSW joint which are mainly affected by tool geometry and process parameters. Recently, some researchers studied the thermal and heat generation aspects of FSSW process. Gerlich and al. [6] measured peak temperature in aluminum and magnesium alloys friction stir spot welds. Two thermocouples were embedded in a welding tool assembly in the experiment. Su and al. [7] have studied energy utilization during FSSW process. Shin and Jung [8] investigated the influences of the plunge speed and plunge depth on the characteristic features of FSSW of bulk metallic glass (BMG) sheets. Fratini and al. [9] studied the friction stir spot welding (FSSW) of AA6082-T6. In particular, process mechanics is highlighted and joint strength is considered in relation to varying the most relevant process parameters. Pan and al. [10] studied the displacement control spot friction weld process of sheets of 6111-T4 aluminum. Kulekci and al. [11] studied the tensile-shear-strength and hardness variations in the weld regions. The results obtained are compared with those derived from the application of traditional resistance spot welding (RSW). Baek and al. [12] examined the effect of tool penetration depth on the microstructures and mechanical properties of FSSW joints of galvanized steel. Abu Mowazzem and al. [13] investigated experimentally the welding process, microstructure and failure of the FSSW joint of 409L Stainless Steels.

Bilici [14] investigated the effects of tool geometry and properties on friction stir spot welding properties of polypropylene sheets. Four different tool pin geometries, with varying pin angles, pin lengths, shoulder diameters and shoulder angles are used for friction stir spot welding. Bilici and Yukler [15] investigated the effects of the welding parameters on static strength of friction stir spot welds in polymer. Cavaliere and al. [16] analysed the effect of welding parameters on the mechanical and microstructural properties of dissimilar AA6082–AA2024 joints produced by friction stir welding. In this study, the application of friction stir spot welding (FSSW) technique has been initially investigated and the characteristic feature observed was discussed based on the influences of plunge depth and plunge speed of the probe on it.

2. Experimental method

In this investigation, distinct aluminium 6060-T5 sheets were welded using for different parameters. The chemical composition of the aluminium 6060-T5 sheet is presented in Table 1 and the mechanical properties of the sheets are presented in Table 2.

* UNIVERSITY OF SIDI BEL ABBÈS, LABORATORY OF MATERIALS AND REACTIVE SYSTEMS – LMSR. BP. 89, CITY LARBI BEN MHIDI. SIDI BEL ABBES, ALGERIA
** DJILLALI LIABES UNIVERSITY OF SIDI BEL-ABBES, MECHANICS AND PHYSICS OF MATERIALS LABORATORY, BP89 CITY LARBI BEN M'HIDI, SIDI BEL-ABBES, ALGERIA
# Corresponding author: m_merzoug01@yahoo.fr

To start the welding process, two sheets of aluminium 6060-T5 are joined in a lap configuration as shown in Fig. 1.

TABLE 1

Chemical composition of 6060 T5 aluminum alloy (mass fraction, %)

%	Si	Fe	Cu	Mn	Mg	Cr	Zn	Ti
Min	0.03	0.10			0.35			
Max	0 60	0.30	0.10	0.10	0.60	0.05	0.15	0.10

TABLE 2

Mechanical properties of 6060 T5 aluminum alloy

E (MPa)	*Rp* (MPa)	*Rm* (MPa)	*A* (%)	*v*	*d* (g/cm^3)	Fusion T° (°C)	*λ* (W/m°C)	*Cp* (J/Kg°C)
69500	110	150	14	0.33	2.70	605-665	200	945

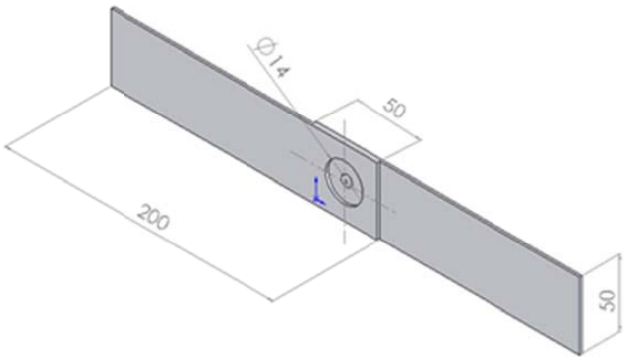

Fig. 1. Tensile-shear testing specimen

The upper test coupon was 2 mm. Their dimensions were 200×50 mm. They were welded in a lap joint with 50 mm cover. Fig. 1. The lower sheet is put on a supporting plate while a rotating tool, as shown in Fig. 3, presses the upper sheet. The back plate supports the downward force of the rotating pin while the rotational speed of the pin results in softening the aluminium but not melting it.

Welds were made using a mixing tool, in a high-alloy steel (X210Cr12), (Fig. 2), with a threaded cylindrical pin (5 mm diameter and 3.95 mm in length) and shoulder (14 mm diameter). Table 3 gives the chemical composition of this material. (Fig. 3a) shows the fixture that was designed to clamp the specimen using a cover plate. (Fig. 3b) shows a schematic of an extracted tool and two welded sheets after welding. The actual bonding diameter for the weld is denoted as Dc. The plunge depth H, and the diameter of the weld, Dc, will depend upon the processing parameters.

TABLE 3

Chemical composition (%) (X210Cr12)

C	Si	Mn	P max	S max	Cr
1.9 to 2.2	0.1 to 0.6	0.2 to 0.6	0.03	0.03	11 to 13

Mechanical properties are *Rm* = 870 MPa and *HB* = 30.

Rotation speed, plunge speed and dwell time were studied. Table 4 lists the parameters used for all welding FSSW process.

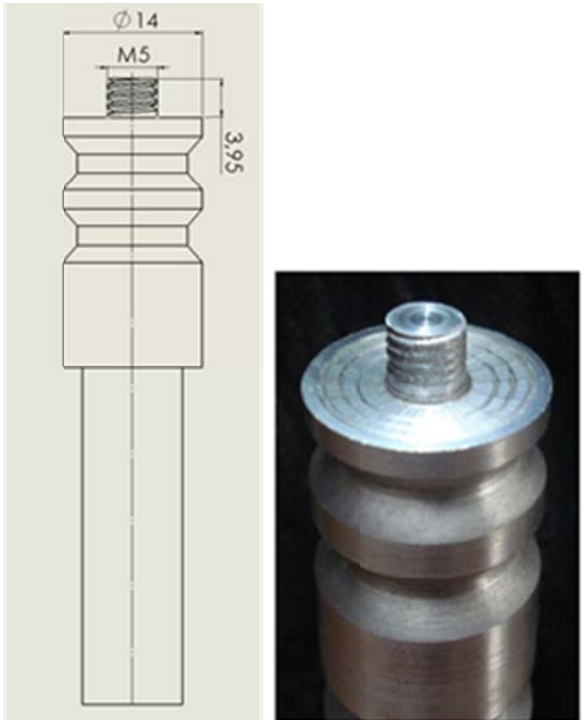

Fig. 2. The rotating tool

(a)

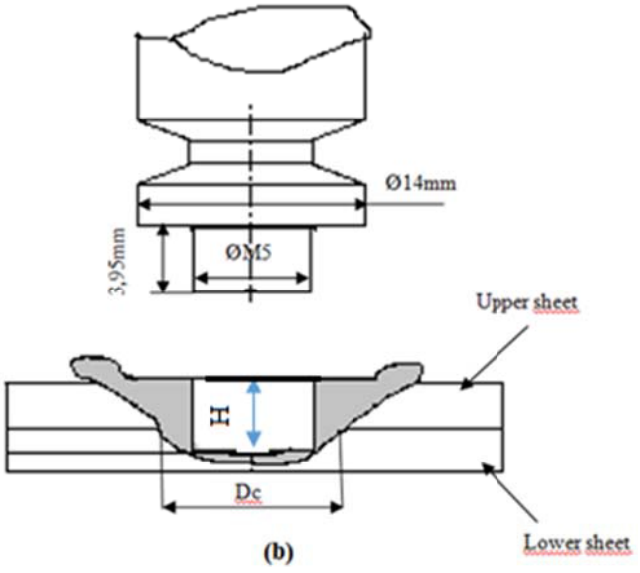

(b)

Fig. 3. (a) spot friction welding system; (b) A schematic of an extracted tool and two welded sheets after welding

We varied the tool penetration speed into the material to be welded from 16 to 31.5 mm/min and the tool rotation speed from 1000 to 2000 rpm.

Thermocouples used in this study are placed between 12 and 15 mm from the center of the stir zone (SZ) for predicting the temperature during the welding operation (Fig. 4).

TABLE 4

Welding parameters with FSSW

Test	Rotation speed (tr/min)	Plunge speed (mm/min)	Welding time (s)	Distance from the center of pin (mm)	Tempe-rature
1	+1400	–16	–48	–12	292
2	–1000	–16	–48	–12	321
3	+1400	+20	–48	–12	317
4	–1000	+20	–48	–12	320
5	+1400	–16	+53	–12	315
6	–1000	–16	+53	–12	305
7	+1400	+20	+53	–12	331
8	–1000	+20	+53	–12	299
9	+1400	–16	–48	+15	276
10	+1000	–16	–48	+15	330
11	–1400	+20	–48	+15	312
12	+1000	+20	–48	+15	335
13	–1400	–16	+53	+15	320
14	+1000	–16	+53	+15	322
15	+1400	+20	+53	+15	321
16	–1000	+20	+53	+15	325

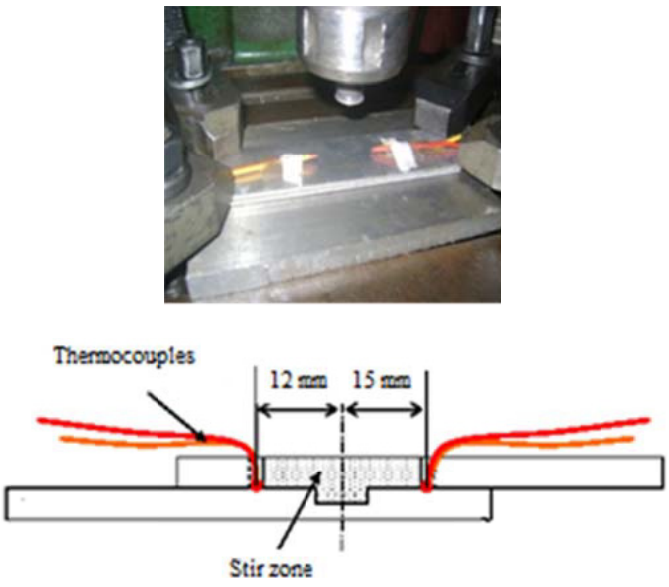

Fig. 4. Position of thermocouples used in this investigation

2.1. Analysis of variance (ANOVA)

Analysis of variance (ANOVA) test was performed to identify the process parameters that are statistically significant. The purpose of the ANOVA test is to investigate the significance of the process parameters, which affect the temperature of FSSW joints. In addition, the rotational speeds used have a significant effect on temperature. Usually, the change of the process parameter has a significant effect on the quality characteristics, when the rotational speed is high. The results of ANOVA indicate that the considered process parameters are highly significant factors affecting the temperature of FSSW joints in the order of rotational speed, plunge speed and welding time.

2.2. Mathematical modeling

The general form of a quadratic polynomial which gives the relation between response surface 'y' and the process variable 'x' under investigation is given in equation. The values of the coefficients of the polynomials were calculated by multiple regression method. In the experimental research, modeling and adaptive control of multifactor processes the rotatable central composite design (RCCD) of experiments is very often used because it offers the possibility of optimization Eq (1).

In the present work, rotational speed, plunge speed, welding time and distance from the center of pin have been considered as the welding parameters. The response temperature can be expressed as a function of process parameters Eq (2).

FSSW has been carried out based on four factors two levels central composite rotatable design with full replications technique. Table 4 shows the 16 sets of coded conditions used to form the design matrix. The data in Table 5 is used as input data to form a mathematical equation by the design of experiment method and response surface methodology in Mini-tab software.

TABLE 5

Design matrix and experimental results

N°	Rotation speed (tr/min)	Plunge speed (mm/min)	Welding time (s)	Distance from the center of pin (mm)	Tempe-rature
1	+1	–1	–1	–1	292
2	–1	–1	–1	–1	321
3	+1	+1	–1	–1	317
4	–1	+1	–1	–1	320
5	+1	–1	+1	–1	315
6	–1	–1	+1	–1	305
7	+1	+1	+1	–1	331
8	–1	+1	+1	–1	299
9	+1	–1	–1	+1	276
10	–1	–1	–1	+1	330
11	+1	+1	–1	+1	312
12	–1	+1	–1	+1	335
13	+1	–1	+1	+1	320
14	–1	–1	+1	+1	322
15	+1	+1	+1	+1	321
16	–1	+1	+1	+1	325

2.3. Tensile test

The objective of our work is to study the tensile stress of friction stir welded plates of" aluminum alloy 6060-T5 with

Fig. 5. An example of tensile shear test specimens

a rotating tool at various speeds and diving. Specimens used were prepared as shown in Fig. 5. The load and displacement were simultaneously recorded during the test. All tensile tests were performed at a constant crosshead displacement rate of 10 mm/min. The maximum load and failure location were recorded for each specimen

$$y = a_0 + \sum_{i=1}^{4} a_i x_i + \sum_{1 \le i < j \le 4} a_{ij} x_i x_j + \sum_{i=1}^{4} a_{ii} x_i^2 + e \qquad (1)$$

$$Y = a_0 + a_1 X_1 + a_2 X_2 + a_3 X_3 + a_4 X_4 + I_{12} X_1 X_2 + \\ + I_{13} X_1 X_3 + I_{14} X_1 X_4 + I_{23} X_2 X_3 + I_{34} X_3 X_4 \qquad (2)$$

3. Results and discussions

3.1. Microhardness profile

Fig. 6 shows the evolution of the hardness for different plunging speeds *Vp* and different rotations speed ω. We observe a decrease of the micro hardness in the heat-affected zone (HAZ) and hardening in the thermo-mechanically affected zone (TMAZ) and the MZ .D.A. Wang [17]. The decrease of the microhardness is due to a small heat distortion during welding, which increases the density of dislocations.

Fig. 6 illustrates the variation of the HV of the nugget compared to base metal according speed rotation and plunging speed. We remark a stable values obtained with 1000 rpm and 16mm/min. This stability can satisfy the welded assembly by Merzoug et al. [18].

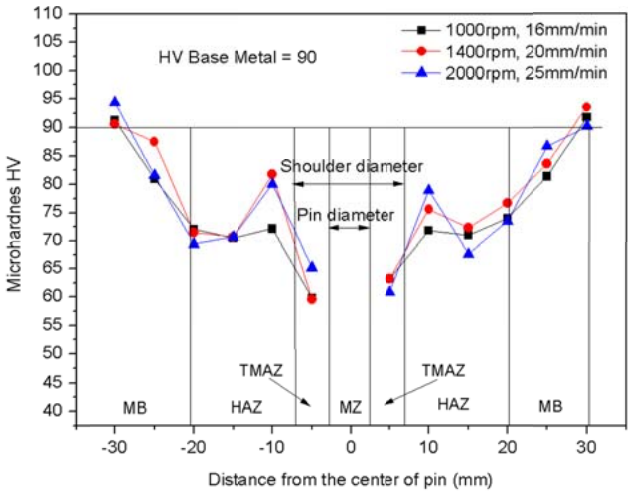

Fig. 6. Variation in micro hardness vs. distance from weld center

3.2. Macroscopic study

Based on the observations of the FSSW macrostructures, the weld zone of a FSSW joint is schematically illustrated in Fig. 7. From the appearance of the weld cross section, two geometrical characteristics of the weld may be identified. The first is the thickness of the weld stir zone stir zone (*x*) which is an indicator of the weld bond area. The weld bond area increases with the stir zone stir zone thickness. The second is the thickness of the upper sheet under the shoulder indentation (*y*). These geometrical characteristics determine the strength of a FSSW joint. There are numerous papers concerning the FSSW parameters which affect the joint geometry and the weld strength [14].

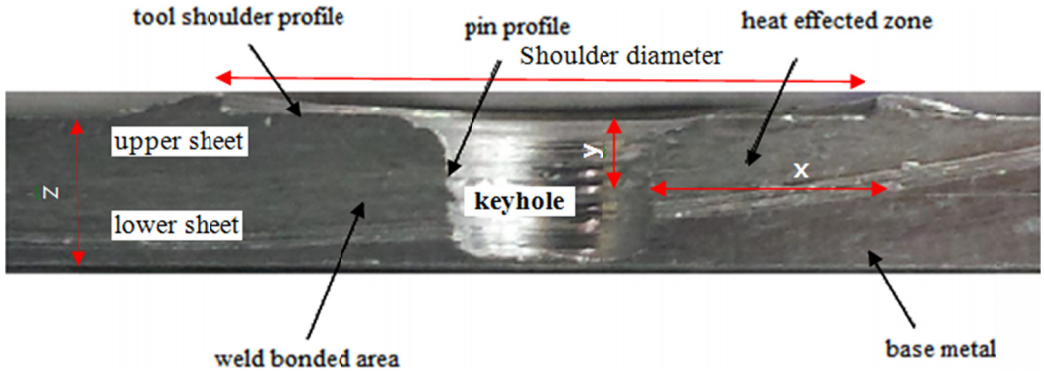

Fig. 7. Schematic illustration of the cross section of afriction stir spot weld. x*:* stir zone thickness, y *:*the thickness of the upper sheet and z*:* total materials thickness

3.3. Temperature profiles

Fig. 8 shows temperature profiles with varying tool speeds. The maximum temperature at tool speed (1000 rpm) and almost identical at higher tool speeds (1400 rpm). For example, at 1000 and 1400 rpm the maximum temperatures were 300 and 350°C respectively.

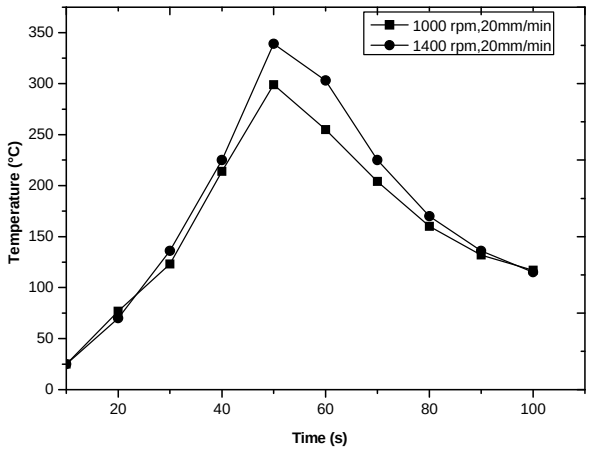

Fig. 8. Temperature profile measured

Fig. 9 presents data points, represented by the open square symbols, for relative temperature vs ω. It can be seen that the temperature increases with increasing rotational speed at a constant welding speeds tool. It can be inferred that the temperature is inversely proportional to the rotational speed [19].

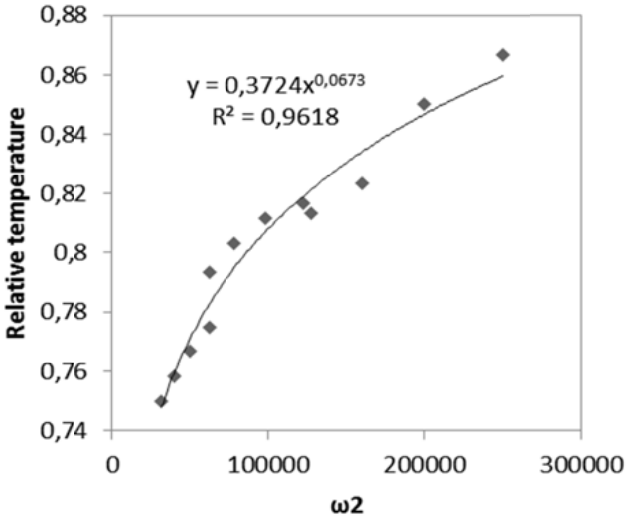

Fig. 9. Relative temperature vs. ω^2 experimental results and modeling

3.4. Tension-shear tests

Fig. 10 shows a typical load-displacement curve of a spot welding by friction stir. There is on this curve, the parameters plunge speed = 16 mm / min and rotational speed = 1000 rpm, give the best tensile strength. The lowest is obtained for plunge speed = 25 mm / min and rotational speed = 2000 rpm. To analyze

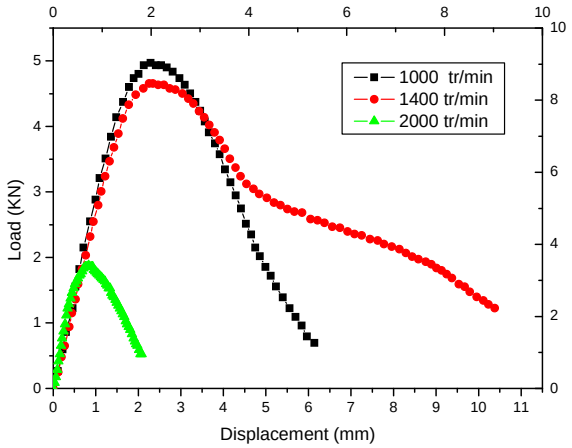

Fig. 10. Typical load curve – displacement

the evolution of the mechanical with the welding parameters, averaged over several trials is calculated.

In tests shear. Lathabai [20] and Tozaki [21] showed that the friction stir welding presents two failure modes. The first is the shear fracture or the interfacial fracture which comes from the transition point and propagates to the free edge of the hole of the pin of the tool and the second is the mixed mode fracture. This failure mode is also encouraged by thinning of the top sheet at the edge of the tool shoulder, due to the shoulder plunge. Klobčar et al. [22]. Failure by mode III is associated with moderately higher shear strength and far larger fracture energy compared to mode II. Klobčar et al. [22].

For the tensile/ shear samples welded at the rotational speed of 1000 rpm, the crack initiates in the tip of the hook and then propagates along the hook. In addition, as mentioned above, when the joint is subject to the external loading, the upper sheet bends upward and the lower sheet bends downward, which leads to the nugget rotation seen in Fig. 11. As a result of the nugget rotation, the load component perpendicular to the nugget is generated and then induces the crack to grow along the thickness direction. Uematsu [23].

Fig. 11. Shear specimen during the tensile test

Fig. 12 shows that the deformation has not occurred in the weld interface, total shear started on the side of the melting zone in the heat affected zone. The upper plate is completely separated from the lower plate

3.5. Development of the mathematical model

In this investigation, the response surface methodology was used to predict maximum temperature of aluminium 6060 T5 in terms of the friction stir spot welding process parameters. The application of response surface methodology to a welding procedure can be dealt elsewhere. The temperature of friction stir spot-welded is a function of the welding parameters such as tool rotational speed (N) , plunge speed (Pw), welding time (Time), and distance from the center of pin (d) and it can be expressed as,

$$\text{Temperature} = f(N, Pw, Time, d),\ y = f(X_1, X_2, X_3, X_4)$$

After omitting insignificant factors, the mathematical model is obtained as shown in Eq (3).

The theoretical values derived by the mathematical model represented by the straight-line and the experimental values represented by the point cloud. The deviation of these points with respect to the right represents the calculated difference or the residue. This indicates that a high correlation exists among the experimental values and the predicted values. The normal probability plot for temperature rate reveals that the residuals are falling on the straight line, which means the errors are distributed normally. All of this indicates an excellent suitability of the regression model (Fig. 13).

3.6. Effect of FSSW process parameters

From the results of statistical analysis it can be seen that out of the four welding parameters undertaken for the study, the tool rotational speed and dwell time have the maximum contribution to both the temperature variation and the lap shear strength of the welded specimens. Hence, these are selected for further analysis and inferences. Experimental treatments that were conducted at different tool rotational speeds: 1000 rpm and 1400 rpm, while the plunging rate, tool plunge depth and dwell time were constant were chosen to study the effect of variation in tool rotational speed on the transient temperature distribution within the welding zone. The effect of welding parameters on the

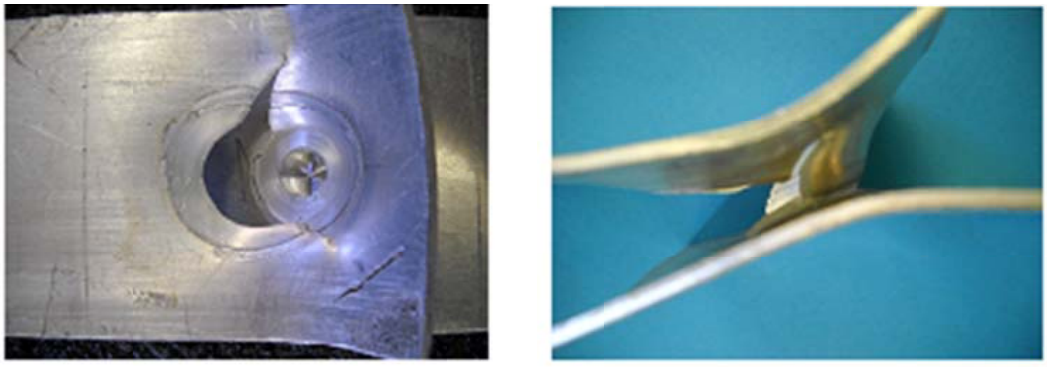

(a) lose-up top view of the upper sheet (b) close-up side view of the joint

Fig. 12. Tensile/shear mixed fracture observed with the parameter: 1000 rpm and 16 mm/min

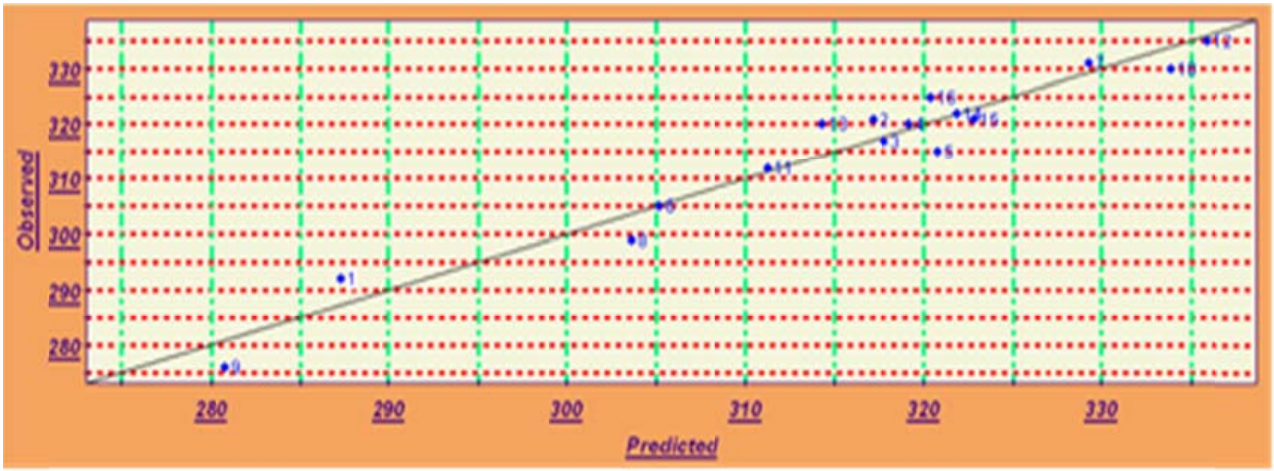

Fig. 13. Normal probability plot of regression

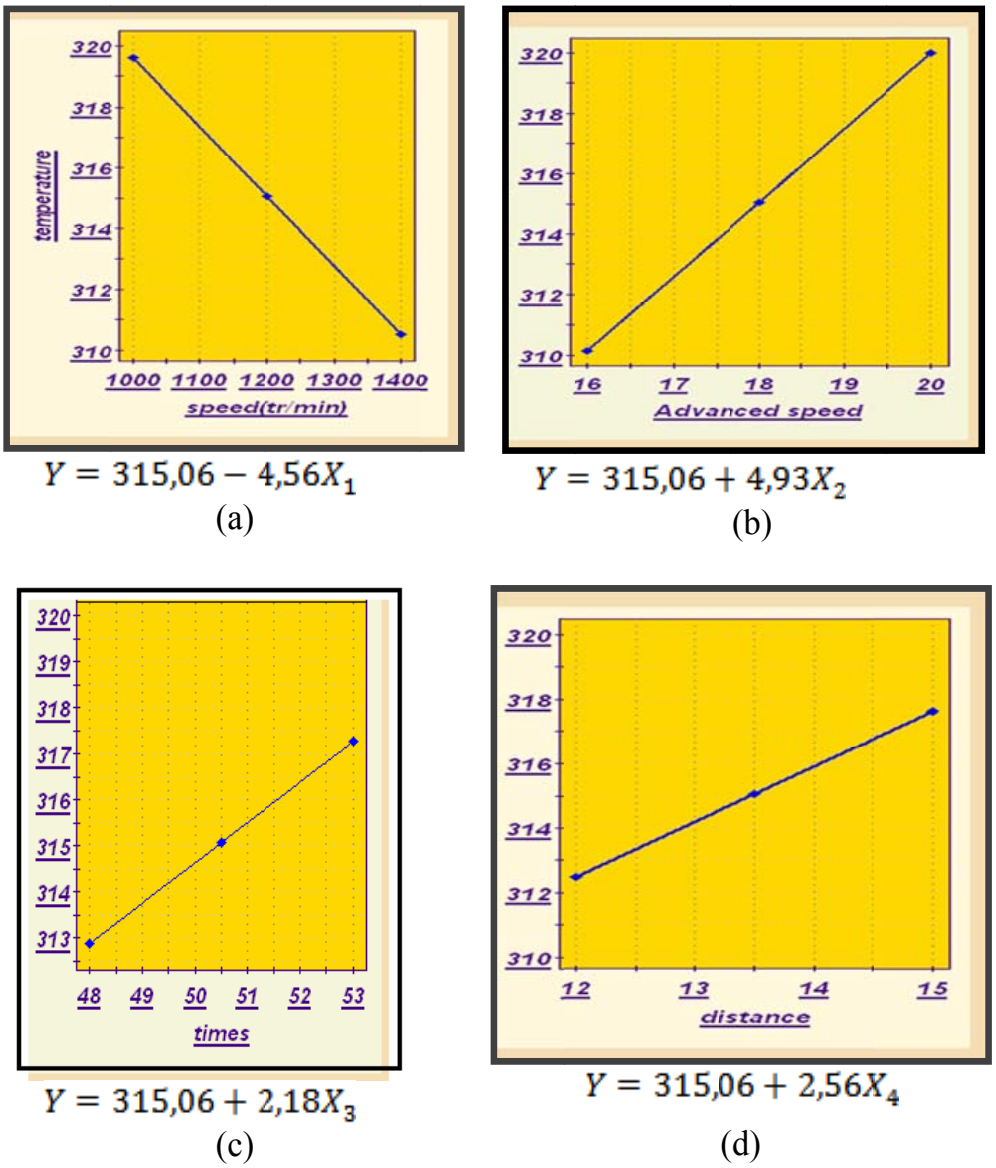

Fig. 14. Effect of welding parameters on temperature variation during FSSW

transient temperature distribution is shown graphically in Fig. 14. (Fig. 14a) shows the effect of the rotational speed is important in decreasing the speed of rotation, the temperature increases toward the maximum value. At a rotation of 1000 rpm, the temperature reaches 320°C and 312°C to devoid the rotational speed for the same 1400 tr/min welding speed 20 mm / min. Welding speed also plays a very important role in this phenomenon but it faith towards increasing the temperature goes with the growth of this speed. (Fig. 14b) shows the difference of temperature, 310°C to 321°C and 16mm/min at 20 mm / min which confirms that the slope of the line is positive. The curve in (Fig. 14c) is upward, in other words over time tends to increase and its maximum value, the more the temperature increases, but with a small slope. That is to say the temperature increases from 313°C for a time of 48 s at 317°C for 53 s. It can be concluded that this affects the variation of the temperature. The (Fig. 14d) shows the influence of the distance. 12 mm A temperature = 314°C whereas for a distance 15 mm the temperature reaches 317°C.

3.6.1. Interaction between feed rates and rotation

The analysis of this step shows the interaction of 04 factors, feed rates (16.5 mm/min and 19.5 mm/min) and speeds (1050 tr/min and 1350 tr/min) while fixing the distance of 15 mm and time 53 s (Fig. 15). The chart below has allowed us to visualize the temperature variation. It is then found that the temperature reaches a maximum value with a 325.2°C and decreases to a minimum value while increasing the speed to the value 1400 tr/min.

3.6.2. Interaction between rotation speeds and time

In this case, the feed speed and the distance is fixed and varies the rotational speed and time. (Fig. 16). Note that the

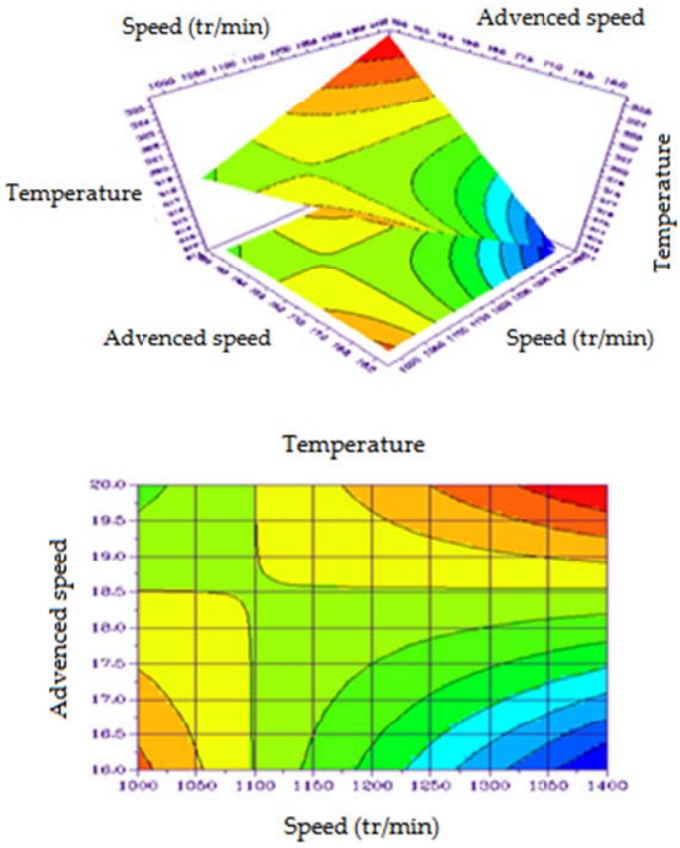

Fig. 15. Interaction between feed rates and rotation: distance being fixed at 15 mm and time 53s

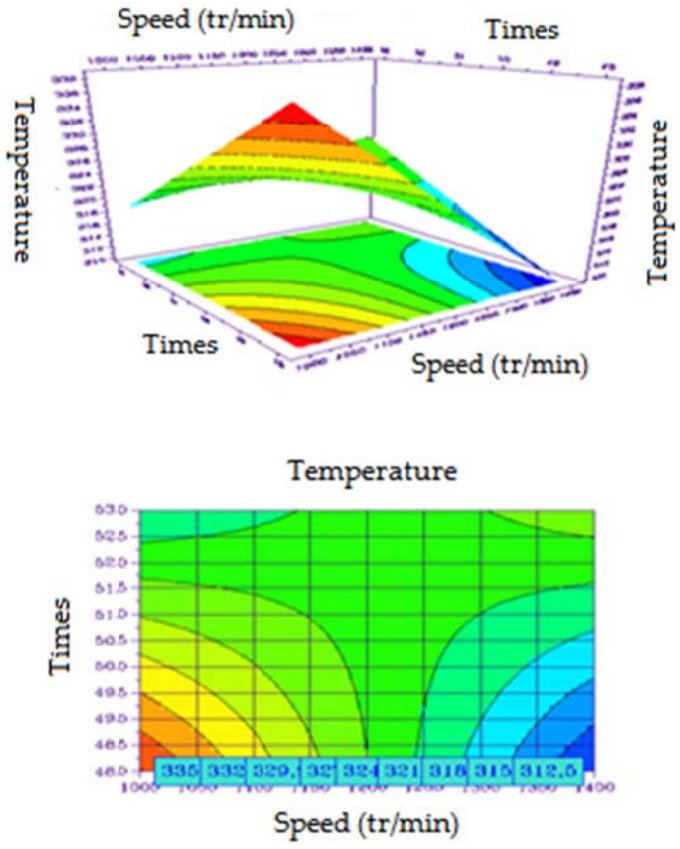

Fig. 16. Interaction between rotation speeds and time: distance being set at 15 mm and the feeding speed to 20 mm/min

temperature takes its maximum value when the rotational speed is minimal. The analysis of the curves also show that temperature is the minimum while approaching 1400 tr/min rotation speed, so the temperature varies directly with the rotational speed against the change of time is not significant.

3.6.3. Interaction between the rotational speed and distance

In this graph (Fig. 17), the surface remains flat, the variation is linear with the linearity of the polynomial. The temperature increases with increasing speed of rotation, the distance in this case has no influence.

3.6.4. Interaction between feed rates and time

The analysis shows that the iso curves (Fig. 18) for a forward kept constant at 16.5 mm / min, the temperature reaches the value 310°C where the time is 53 s. For this, the two factors set to the maximum values (to 20 mm/min feeding speed and the time to 53 s), therefore it can be concluded that the increase of the temperature is linked simultaneously to the increase of both factors.

3.6.5. Interaction between distance and time

The analysis of this graph (Fig. 19) shows that, for a distance equal to the temperature at 16 mm to 311°C if the welding operation lasts 48 s, 53 s at the temperature reached a value of 225°C. By decreasing the distance (12 mm) and setting time to 53 s, the temperature takes its maximum value.

$$Y = 315{,}06 - 4{,}56X_1 + 4{,}93X_2 + 2{,}18X_3 + 2{,}56X_4 + \\ + 4{,}81X_1X_2 + 9{,}06X_1X_3 - 5{,}81X_1X_4 + \\ - 3{,}18X_2X_3 + 2{,}18X_3X_4 \quad (3)$$

4. Conclusions

The FSSW process does not use any external heat source. The dissipation after the mixing of the material and its friction against the tool sufficient to cause a temperature rise to the formation of solder in the solid state. In general, the temperatures reached do not exceed 80% of the melting temperature of the base metal of 6060-T5 aluminium.

This study focuses on the influence of four factors (speed, feed rate, welding time and distance from the point of welding). To predict these effects, the method of experimental design is a tool that, combined with experimental measurements, allows us to understand and control the consequences that can result from the friction stir welding process.

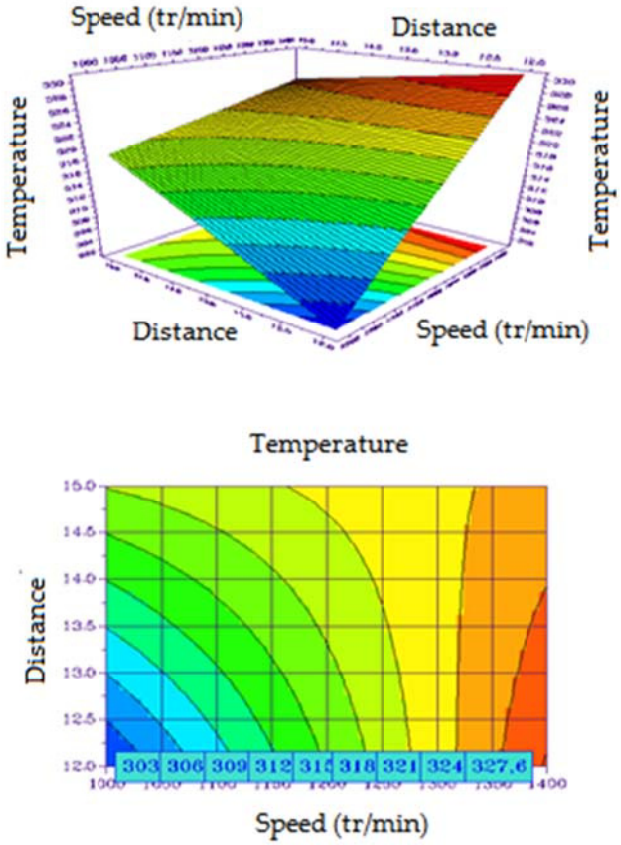

Fig. 17. Interaction between the rotational speed and distance

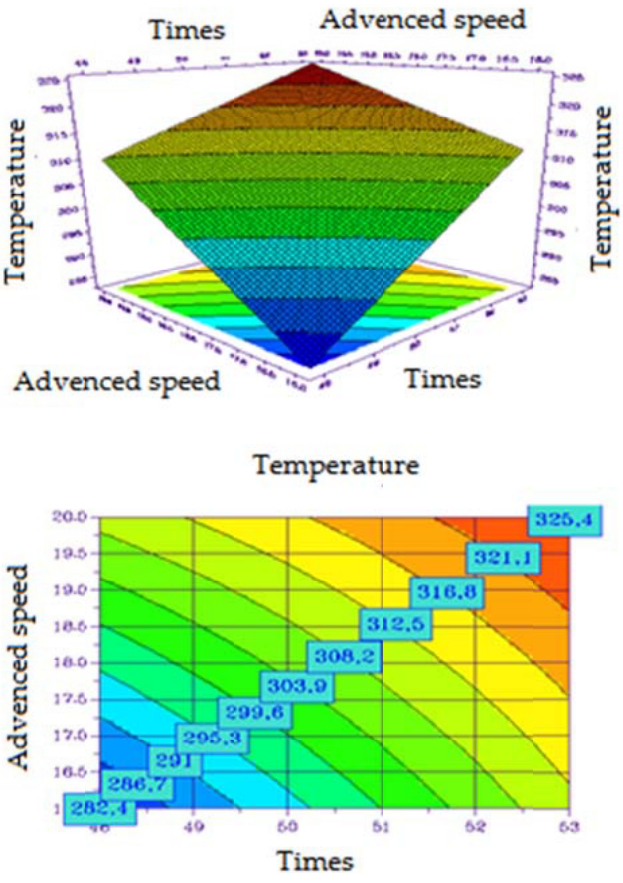

Fig. 18. Interaction between feed rates and time: distance being set at 15 mm and the rotational speed of 1400 tr / min

REFERENCES

[1] P. Lin, S. Lin, J. Pan, T. Pan, L. Nicholson, M. Garman, Microstructures and Failure Mechanisms of Spot Friction Welds in Lap-Shear Specimens of Aluminum 6111-T4 Sheets, Proc. of the SAE. W. Cong. Michigan. (2004).

[2] Z. Feng, M. Santella, S. David, R. Steel, S. Packer, T. Pan, M. Kuo, R. Bhatnagar, Friction Stir Spot Welding of Advanced High-Strength Steels-A Feasibility Study, Proc. of the SAE. Cong, Detroit, MI. (2005).

[3] D. Mitlin, V. Radmilovic, T. Pan, Z. Feng, M. Santella, Structure--Properties Relations in Spot Friction Welded 6111 T4 Aluminum, TMS Ann. Mee, San Francisco (2005).

[4] T. Pan, A. Joaquin, E .Wilkosz, L. Reatherford, J. Nicholson, Z. Feng, M. Santella, Spot Friction Welding for Sheet Aluminum Joining, 5th Int Sym on F S W, P. Threadgill, ed., The W. Inst., Metz, France, Paper No. 11A-1. (2004).

[5] R. Sakano, K. Murakami, K .Yamashita, T. Hyoe, M. Fujimoto, M. Inuzuka, Y. Nagao, H. Kashiki, Development of Spot FSW Robot System for Automobile Body Members, Proc.of the 3rd. Int. S of FSW, Kobe, Japan (2001).

[6] A. Gerlich, P. Su, T. North, Peak Temperatures and Microstructures in Aluminum and Magnesium Alloy Friction Stir Spot Welds, Sc. and Tech. of Wel. and Joi. **10**, 647-652 (2005).

[7] P. Su, A. Gerlich, T. North, G. Bendzsak, Energy Utilization and Generation during Friction Stir Spot Welding, Sc. and Tech. of Wel. and Joi. 163-169 (2006).

[8] S. Hyung-Seop, J. Yoon-Chul, Characteristics of friction stir spot welding of Zr-based bulk metallic glass sheets, J. of Al and Compounds **504S**, S279-S282 (2010).

[9] L. Fratini, A. Barcellona, G. Buffa, D. Palmeri, Friction stir spot welding of AA6082-T6: influence of the most relevant process parameters and comparison with classic mechanical fastening techniques, Pro. of the Ins. of Mec. Eng. **221**, Part B, J. Eng. Man. 1111-1118 (2007).

[10] P. Tsung-Yu, et al, Spot Friction Welding for Sheet Aluminum Joining, F. Mot. Com., Dearborn, Michigan 48124, U.S.A. (2007).

[11] M. Kemal Kulekci, O.E. Ugur Esme, Experimental comparison of resistance spot welding and friction-stir spot welding processes for the en aw 5005 aluminum alloy, MTAEC9 **45** (5) 395 (2011).

[12] S.W. Baek, D.H. Choi, C.Y. Lee, B.W. Ahn, Y.M. Yeon, K. Song, S.B. Jung, Mater. Trans. **51**, 1044 (2010).

[13] Md. Abu Mowazzem Hossain, Md. Tariqul Hasan, S. Tae Hong, M. Miles, H. Cho, H.H. Nam, Friction Stir Spot Welded Joints of 409L Stainless Steels Fabricated by a Convex Shoulder Tool, Met. Mater. Int. **19**, 6, 1243-1250 (2013).

[14] M.K. Bilici, Effect of tool geometry on friction stir spot welding of polypropylene sheets, exp. Poly. Letters **6**, 10, 805-813- to be updated. (2012).

[15] M.K. Bilici, A.I. Yukler, Effects of welding parameters on friction stir spot welding of high density polyethylene sheets, Mater. and D. **33**, 545-550 (2012).

[16] P. Cavaliere, A. De Santis, F. Panella, A. Squillace, Effect of welding parameters on mechanical and microstructural properties

of dissimilar AA6082-AA2024 joints produced by friction stir welding", Mater. and D. **30**, 609-616 (2009).

[17] D.A. Wang. S.C. Lee, Microstructures and failure mechanisms of Friction Stir Spot Welds of aluminium 6061-T6 sheets, J. of Mat. Pro. Tech. **186** (2007).

[18] M. Merzoug, M. Mazari, L. Berrahal, A. Imad, Parametric studies of the process of friction spot stir welding of aluminium 6060-T5 alloys, Mater. Des. **31** (6), 3023-3028 (2010).

[19] R.S. Mishra, Z.Y. Ma, Friction stir welding and processing, Mater. Sci. and Eng. **50**, 1-78 (2005).

[20] S. Lathabai, M.J. Painter, G.M.D. Cantin, V.K. Tyagi, Friction spot joining of an extruded Al-Mg-Si alloy, Scri. Mater. **55**, 899-902 (2006).

[21] Y. Tozaki, Y. Uematsu, K. Tokaji, Effect of tool geometry on microstructure and static strength in friction stir spot welded aluminium alloys, Inter. J. of Mac. Tools and Man. **47**, 2230-2236 (2007).

[22] D. Klobčar, J. Tušek, A. Skumavc, A. Smolej, Parametric study of friction stir spot welding of aluminium alloy 5754, METABK **53** (1) 21-24 (2014).

[23] Y. Uematsu, K. Tokaji, Comparison of fatigue behaviour between resistance spot and friction stir spot welded aluminium alloy sheets, Sci. Technol. Weld. Join. **14**, 62-71 (2009).